RESEARCH ARTICLE

Modeling the Impact of Vaccination and Post-Treatment on Rabies Transmission

Hanif Ullah[1], **Amjid Ali**[1,*] **and Hazrat Younas**[2]

[1] Department of Basic Science and Islamiat, University of Engineering and Technology, Peshawar 25013, Khyber Pakhtunkhwa, Pakistan
[2] Department of Mathematics, University of Malakand, Chakdara 18800, Khyber Pakhtunkhwa, Pakistan

Abstract

Rabies remains a serious public health concern, as dog bites account for the majority of human cases. In this study, we develop a comprehensive mathematical model to investigate the dynamics of rabies transmission by incorporating two key intervention strategies: an asymptotic class (P) and a booster vaccination class (B). The basic reproduction number (R_0) is derived as a threshold parameter that governs whether the disease spreads or dies out, based on a system of nonlinear differential equations. A sensitivity analysis of R_0 is conducted to identify the most influential parameters affecting disease transmission. The results indicate that the transmission rate (β) has a significant impact on R_0, emphasizing the importance of reducing contact between susceptible and infected populations. Stability analysis of both the disease-free and endemic equilibria reveals that the disease can be eradicated when $R_0 < 1$, whereas it persists when $R_0 > 1$. Numerical simulations, performed using the classical Runge–Kutta method, illustrate the comparative effects of vaccination and treatment interventions. The results demonstrate that the inclusion of the booster vaccination class (B) substantially reduces the number of infected individuals compared to the scenario without vaccination. Moreover, the therapeutic class (P) further accelerates recovery and alleviates the overall disease burden. Analysis of varying transmission rates (β) shows that higher values lead to a rapid rise in infection levels, underscoring the necessity for effective intervention strategies in high-contact environments. Overall, the model highlights that integrating booster vaccination and treatment measures within rabies control programs can significantly decrease disease prevalence. The findings of this study provide valuable insights for public health authorities aiming to design efficient strategies for the control and eventual eradication of rabies.

Keywords: rabies, mathematical model, stability, bifurcation, rabies model.

1 Introduction

Humans and other mammals are susceptible to the zoonotic disease rabies, which is caused by a rabies virus. It belongs to the genus Lyssa virus and family

Submitted: 25 October 2025
Accepted: 02 November 2025
Published: 11 December 2025

Vol. 1, **No.** 2, 2025.
10.62762/JNSPM.2025.826101

***Corresponding author:**
✉ Amjid Ali
hanifullahbjr23@gmail.com

Citation
Ullah, H., Ali, A., & Younas, H. (2025). Modeling the Impact of Vaccination and Post-Treatment on Rabies Transmission. *Journal of Numerical Simulations in Physics and Mathematics*, 1(2), 84–97.

Rhabdomancy [1, 2]. Since the virus is found in saliva, the most common method of transmission is through an animal's bite [3]. Dogs are the primary mammals that transmit the rabies virus from other animals to humans, along with bats, skunks, raccoons, foxes, and cats [4]. Peripheral nerves allow rabies to penetrate the central nervous system. The virus causes encephalitis, which results in severe neurological symptoms that worsen over time, such as paralysis of the muscles, anxiety, and aberrant neurological signs [5, 6]. Rabies continues to be a major global health concern, accounting for over 59,000 deaths annually, a large majority of which occur in Africa and Asia [7]. It is true that rabies is a deadly disease, and that once infected, recovery is quite unlikely. In extremely rare instances, rabies virus infections can be recovered from but result in serious neurological impairments Since the illness may cause the patient to suffer from severe physical or mental disability, this is not a true cure in the traditional sense. There have been reported cases of people surviving with no significant neurological aftereffects,despite the fact that they are incredibly rare. The research is incredibly weak when it comes to assertions that an infected animal with rabies can survive. Although there have been fewer cases of rabies in some areas, the disease is still widespread, especially particularly in sub-Saharan Africa and Southeast Asia, where access is restricted to inexpensive vaccinations of livestock and prompt post-exposure prophylaxis [8]. Despite the fact that vaccinations can prevent dog rabies, tens of thousands of people die from the disease annually in low- and middle-income nations [9, 10]. Even if exposed to the virus, rabies is extremely uncommon to strike someone who has received the recommended vaccination against the disease Antibodies that guard against the virus are produced as a result of receiving a rabies vaccination.Before the rabies virus can spread and infect people, these antibodies aid in neutralizing it. Regardless of immunization status,PEP is recommended following possible exposure to rabies against the disease. Antibodies that guard against the virus are produced as a result of receiving a rabies vaccination. Before the rabies virus can spread and infect people, these antibodies aid in neutralizing it. Regardless of immunization status, PEP is recommended following possible exposure to rabies. In order to defend against the virus, PEP entails giving rabies vaccines and, in certain situations, RIG. Preventive and CDC state that people who receive a full pre-exposure vaccination are thought to have long-term immunity and typically do not need booster doses unless they work in a field where exposure to rabies virus is constant, such as veterinary medicine or laboratory work handling samples of the virus. Depending on the environmental circumstances, domestic or wild animals can infect humans with rabies, underscoring the significance of caution and preventive measures [11–14]. Complex dynamics including population density, wildlife populations, and vaccination campaigns all have an impact on the dynamics of rabies transmission. The dynamics of illness, particularly the spread of rabies, have been better understood thanks to mathematical modeling. A number of disease modeling-related topics, including asymptotic stability, media effect, contagion, and treatment techniques, have been the subject of recent research [15, 16]. Specifically. several mathematical models have analyzed the dynamics of rabies transmission and proposed mitigation and control strategies. However, externally imported illnesses are often overlooked in traditional models, despite the fact that they might significantly affect the transmission [17].

Various mathematical models have recently analyzed the dynamics of rabies transmission and proposed control strategies for preventing the disease [18, 19, 23, 27, 28]. However, most traditional models overlook the significant impact of infective immigrants [20], vaccination waning [30], and the role of booster vaccination and asymptomatic carriers — factors that our model explicitly incorporates [30, 31]. Additionally, while optimal control strategies [21] and spatial dispersal effects [23] have been examined in some studies, few integrate vaccination, post-exposure treatment, and immigrant infection within a single framework as we do here. This paper addresses this gap by incorporating the effects of infected immigrants and combining the Routh-Hurwitz criterion, a quadratic Lyapunov function, and a next-generation matrix (NGM) approach. These methods aim to enhance the model's accuracy, dependability, and practicality. Following WHO guidelines, we present a new perspective on modeling the dynamics of animal rabies while ensuring the credibility of the referenced sources. This approach also aims to clarify the common misconception about recovery from rabies, which is often perceived as almost universally fatal.

2 Meterial and Methods

An analysis of animal rabies disease dynamics with infective animals immigrants is conducted using a nonlinear mathematical model of

Susceptible-Vaccinated-Exposed-Infected-Recovered. The flow of individuals between different compartments is illustrated in Figure 1, which presents the proposed model's structure. There are seven subgroups in the model: Susceptible S(t), Vaccinated V(t), Exposed E(t), Infected I(t), Booster vaccinated B(t) and Aysomptotic P(t), S(t) is a term used to describe animals who do not have rabies but may get infections if they come into contact with an infected animal; E(t) refers to animals who have become infected with rabies virus but are not infectious; An animal with vaccinated status V (t) is one that has been vaccinated from a population of susceptible animals; an animal with infected virus I(t) is one that is infectious; an animal with recovered status R(t) is one that has recovered from rabies infection either naturally or through treatment; Booster B(t) Individuals who have received a booster dose for the purpose of maintaining their immunity; Asymptomatic P(t) An infected individual who does not exhibit symptoms. A_h, Recruitment rate of new individuals into the population, α_1, Vaccination rate, α_2, Rate of decline in vaccine immunity, α_3 , Vaccine failure rate, β , Transmission rate, δ_1, Progression rate from exposed to progressed class, δ_2, Progression rate from exposed to infectious class, δ_3, Progression rate from progressed to infectious class, γ_1, Asymptotic rate from exposed class, γ_2, Recovery rate from Asymptotic class, γ_3, Recovery rate from progressed class, K, Natural death rate, m, Disease-induced mortality rate η, Rate of recovered individuals becoming susceptible again.

$$\begin{cases} \frac{dS}{dt} = A_h + \alpha_2 V + \eta R - (\alpha_1 + K)S \\ \frac{dE}{dt} = \beta SI + \alpha_3 V - (\delta_1 + \delta_2 + \gamma_1 + K)E \\ \frac{dI}{dt} = \delta_2 E + \delta_3 P - (K + m)I \\ \frac{dV}{dt} = \alpha_1 S - (\alpha_2 + \alpha_3 + K)V \\ \frac{dB}{dt} = \gamma_1 E - (\gamma_3 + K)B \\ \frac{dP}{dt} = \delta_1 E - (\delta_3 + \gamma_3 + K)P \\ \frac{dR}{dt} = \gamma_3 P + \gamma_2 B - (K + \eta)R \end{cases} \tag{1}$$

3 Well-Posedness of the Model

The well-posedness of a mathematical model refers to the existence, uniqueness, and stability of solutions to the model's equations (1).

3.1 Positivity of Solutions

Theorem: *The solution to the system 1 with non-negative conditions is non-negative.*

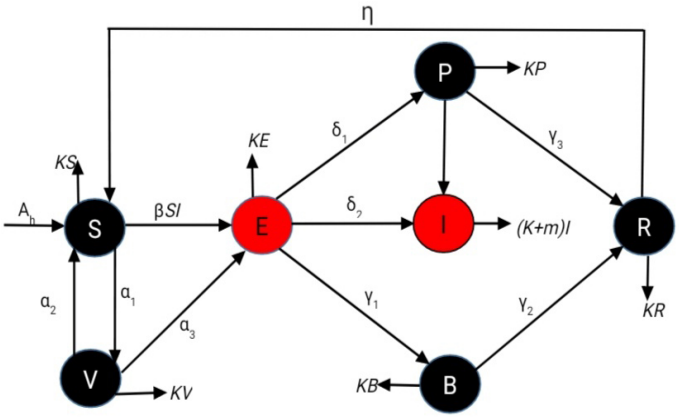

Figure 1. Flow-chart of the proposed model.

Proof: We suppose that there exists $t_0 > 0$ such that $S(t_0) < 0$. From the Intermediate Value Theorem, there exists $t_1 \in [0, t_0]$ such that $S(t_1) = 0$. From Equation (1), we have

$$\frac{dZ(t)}{dt} = A_h + \alpha_2 V + \eta R - (\alpha_1 + K)S, \tag{2}$$

$$\frac{dS(t)}{dt} \geq -(\alpha_1 + K)S \geq 0. \tag{3}$$

The 1st order differential equation can be solved as follows:

$$\text{IF} = e^{\int((\alpha_1+K)S)dt}, \tag{4}$$

$$\begin{aligned} S(t) \cdot \text{IF} &\geq \int \text{IF}(0)\, dt + C, \\ S(t) \cdot e^{\int_0^t((\alpha_1+K)S)dt} &\geq 0, \end{aligned} \tag{5}$$

Putting $S(0) = S_0$, we get

$$\begin{aligned} S(t) \cdot \left(e^{\int_0^t((\alpha_1+K)S)dt}\right) &\geq S_0, \\ S(t) \geq S_0 \left(e^{-\int_0^t((\alpha_1+K)S)dt}\right). \end{aligned} \tag{6}$$

For all $t_1 \in [0, t]$, $S(t) \geq 0$ for $t \geq t_1$ since $t > t_1$, $S(0) \geq 0$, and this contradicts the initial assumption. Thus $S(t) \geq 0$ for $t > 0$. The solutions of the system are non-negative. The same principle is applicable to E, I, V, B, P, R, and we conclude that the solutions of the system are non-negative. □

Restrictions of the Suggested Model

Let's define the total population $N(t)$ as the sum of all compartments in order to test boundedness:

$$N(t) = S(t) + E(t) + I(t) + V(t) + B(t) + P(t) + R(t).$$

$$\frac{dN}{dt} = \frac{dS}{dt} + \frac{dE}{dt} + \frac{dI}{dt} + \frac{dV}{dt} + \frac{dB}{dt} + \frac{dP}{dt} + + \frac{dR}{dt} \quad (7)$$

$$\begin{aligned}\frac{dN}{dt} &= A_h + \alpha_2 V + \eta R - (\alpha_1 + K)S \\ &+ \beta SI + \alpha_3 V - (\delta_1 + \delta_2 + \gamma_1 + K)E \\ &+ \delta_2 E + \delta_3 P - (K + m)I \\ &+ \alpha_1 S - (\alpha_2 + \alpha_3 + K)V \\ &+ \gamma_1 E - (\gamma_3 + K)B \\ &+ \delta_1 E - (\delta_3 + \gamma_3 + K)P \\ &+ \gamma_3 P + \gamma_2 B - (K + \eta)R.\end{aligned}$$

The dynamics of $N(t)$ may be obtained by adding together all the equations:

$$\frac{dN}{dt} = A_h - KN.$$

In this case, the natural death rate is represented by K and the recruiting rate by A_h. This formula may be simplified to:

$$\frac{dN}{dt} = A_h - KN.$$

This differential equation has the following solution:

$$N(t) = \frac{A_h}{K} + \left(N(0) - \frac{A_h}{K}\right) e^{-Kt}.$$

The exponential term disappears when $t \to \infty$, and the whole population $N(t)$ becomes closer:

$$N(t) \to \frac{A_h}{K}.$$

This suggests that $\frac{A_h}{K}$, a positive constant, bounded the population as a whole, $t \to \infty$.

Each compartment (that is, S, E, I, V, B, P, and R) is bounded since the entire population $N(t)$ is bounded and each compartment represents a non-negative fraction of the population. The suggested model has bounds. The whole population $N(t)$, which approaches the finite limit $\frac{A_h}{K}$ as $t \to \infty$, bounded all state variables $S(t)$, $E(t)$, $I(t)$, $V(t)$, $B(t)$, $P(t)$, and $R(t)$. As a result, the model is limited and biologically possible.

4 Invariant Region

A collection in which the solutions persist for all time $t \geq 0$ is known as a *invariant region* for a system of differential equations. Stated differently, the system will remain inside the region in which it begins and remains during all subsequent eras.

$$\Omega = \left\{ (S, E, I, V, B, P, R) \in \mathbb{R}^7_+ \,\middle|\, N(t) \leq \frac{A_h}{K} \right\} \quad (8)$$

5 Disease-Free Equilibrium Point

In epidemiological modeling, the *disease-free equilibrium* (*DFE*) represents a state in which there are no infections within the population. At this point, the number of infectious individuals is zero, indicating that the disease has been completely eradicated from the community.

The disease-free equilibrium for the given model is expressed as

$$E_0 = (S^0, E^0, T^0, V^0, B^0, P^0, R^0),$$

where

$$E_0 = \left(\frac{(\alpha_2+\alpha_3+K)V^0}{\alpha_1},\ 0,\ 0,\ \frac{\alpha_1 A_h}{((\alpha_1+K)(\alpha_2+\alpha_3+K)-\alpha_1\alpha_2)},\ 0,\ 0,\ 0 \right).$$

Mathematically, the disease-free equilibrium is *locally asymptotically stable* when the basic reproduction number $R_0 \leq 1$. In this case, each infected individual produces, on average, less than or equal to one new infection, causing the disease to eventually die out. Conversely, if $R_0 > 1$, the infection can invade the population, leading to disease persistence or an epidemic outbreak.

6 Basic Reproduction Number (R_0)

The basic reproduction number, denoted by R_0, is a key threshold parameter in epidemiology that determines the potential for disease transmission within a population. It represents the average number of secondary infections produced by a single infectious individual in a completely susceptible population. In other words, R_0 quantifies the expected number of new infections generated by one infected individual during the infectious period. The value of R_0 plays a crucial role in determining the persistence or elimination of a disease. Specifically, if $R_0 < 1$, the infection will eventually die out, and no epidemic will occur among humans. Conversely, if $R_0 > 1$, the infection can invade the population and lead to an epidemic outbreak. Therefore, appropriate

control and containment strategies are required to prevent the spread of the disease when $R_0 > 1$. The basic reproduction number R_0 serves as an important measure for understanding the dynamics and future behavior of the Rabies model (18). Numerous studies have investigated the computation of R_0 for different epidemic models [15, 16]. In this study, we apply the next-generation matrix method [17] to derive the expression for R_0 corresponding to the proposed model (1). To this end, we consider the infected compartments of the system (1) and construct the matrices F and V in accordance with the next-generation approach outlined in [22, 31].

$$\begin{cases} \beta SI + \alpha_3 V - (\delta_1 + \delta_2 + \gamma_1 + K)E \\ \delta_2 E + \delta_3 P - (K + m)I \\ \alpha_1 S - (\alpha_2 + \alpha_3 + K)V \\ \delta_1 E - (\delta_3 + \gamma_3 + K)P \end{cases}$$

$$F = \begin{pmatrix} \beta SI \\ 0 \\ 0 \\ 0 \end{pmatrix}, \quad F^* = \begin{pmatrix} o & \beta S^0 & 0 & 0 \\ 0 & 0 & 0 & 0 \\ 0 & 0 & 0 & 0 \\ 0 & 0 & 0 & 0 \end{pmatrix}$$

$$V = \begin{pmatrix} -\alpha_3 V + (\delta_1 + \delta_2 + \gamma_1 + K)E \\ -\delta_2 E - \delta_3 P + (K + m)I \\ -\alpha_1 S + (\alpha_2 + \alpha_3 + K)V \\ -\delta_1 E + (\delta_3 + \gamma_3 + K)P \end{pmatrix},$$

$$V^* = \begin{pmatrix} A_1 & 0 & -\alpha_3 & 0 \\ -\delta_2 & \kappa + m & 0 & \delta_3 \\ 0 & 0 & \kappa + \alpha_2 + \alpha_3 & 0 \\ -\delta_1 & 0 & 0 & \kappa + \gamma_3 + \delta_3 \end{pmatrix},$$

where $A_1 = \kappa + \gamma_1 + \delta_1 + \delta_2$

$$V^{*-1} = \begin{pmatrix} \frac{1}{\kappa+\gamma_1+\delta_1+\delta_2} & 0 & A_3 & 0 \\ -Z_1 & \frac{1}{\kappa+\mu} & j_1 & Z_3 \\ 0 & 0 & \frac{1}{\kappa+\alpha_2+\alpha_3} & 0 \\ j_2 & 0 & A_2 & \frac{1}{\kappa+\gamma_3+\delta_3} \end{pmatrix},$$

where

$A_2 = \frac{\kappa\alpha_3\delta_1 + \mu\alpha_3\delta_1}{(\kappa+\mu)(\kappa+\alpha_2+\alpha_3)(\kappa+\gamma_1+\delta_1+\delta_2)(\kappa+\gamma_3+\delta_3)}$,

$A_3 = \frac{\kappa\alpha_3 + \mu\alpha_3}{(\kappa+\mu)(\kappa+\alpha_2+\alpha_3)(\kappa+\gamma_1+\delta_1+\delta_2)}$,

$Z_1 = \frac{\kappa\delta_2 + \gamma_3\delta_2 + \delta_1\delta_3 + \delta_2\delta_3}{(\kappa+\mu)(\kappa+\gamma_1+\delta_1+\delta_2)(\kappa+\gamma_3+\delta_3)}$,

$Z_2 = \frac{\beta S(\kappa\alpha_3\delta_2 + \alpha_3\gamma_3\delta_2 + \alpha_3\delta_1\delta_3 + \alpha_3\delta_2\delta_3)}{(\kappa+\mu)(\kappa+\alpha_2+\alpha_3)(\kappa+\gamma_1+\delta_1+\delta_2)(\kappa+\gamma_3+\delta_3)}$

$Z_3 = \frac{\delta_3}{(\kappa+\mu)(\kappa+\gamma_3+\delta_3)}$,

$j_1 = \frac{\kappa\alpha_3\delta_2 + \alpha_3\gamma_3\delta_2 + \alpha_3\delta_1\delta_3 + \alpha_3\delta_2\delta_3}{(\kappa+\mu)(\kappa+\alpha_2+\alpha_3)(\kappa+\gamma_1+\delta_1+\delta_2)(\kappa+\gamma_3+\delta_3)}$,

$j_2 = \frac{\delta_1}{(\kappa+\gamma_1+\delta_1+\delta_2)(\kappa+\gamma_3+\delta_3)}$,

$$F^* V^{*-1} = \begin{pmatrix} -A_4 & \frac{\beta S}{\kappa+m} & Z_2 & \frac{\beta S^0 \delta_3}{(\kappa+\mu)(\kappa+\gamma_3+\delta_3)} \\ 0 & 0 & 0 & 0 \\ 0 & 0 & 0 & 0 \\ 0 & 0 & 0 & 0 \end{pmatrix}$$

where $A_4 = \frac{\beta S^0(-\kappa\delta_2 - \gamma_3\delta_2 - \delta_1\delta_3 - \delta_2\delta_3)}{(\kappa+\mu)(\kappa+\gamma_1+\delta_1+\delta_2)(\kappa+\gamma_3+\delta_3)}$,

$$R_0 = \frac{\beta A_h\,(B_1)\,(\kappa\delta_2 + \gamma_3\delta_2 + \delta_1\delta_3 + \delta_2\delta_3)}{(\kappa+\mu)\,(\kappa+\gamma_1+\delta_1+\delta_2)\,(\kappa+\gamma_3+\delta_3)\,B_2) - \alpha_1\alpha_2} \tag{9}$$

where $B_1 = \alpha_2 + \alpha_3 + \kappa$ and $B_2 = (\alpha_1 + \kappa)(\alpha_2 + \alpha_3 + \kappa)$. Equation 18 explicitly shows that R_0 is directly proportional to the transmission rate β and the progression rate δ_2. The three-dimensional surface plot in Figure 2 visualizes how R_0 responds to simultaneous variations in these critical parameters.

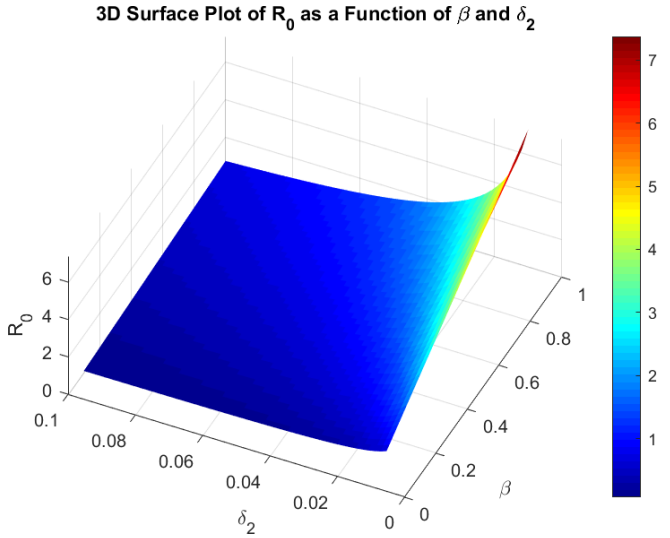

Figure 2. δ_2, and β.

Discussion

High R_0 Values

Regions with high R_0 values indicate conditions that are prone to outbreaks. In such situations, effective control strategies are essential to prevent the rapid spread of infection. Possible measures include:

- Reducing the contact rate, (see Figure 3) (A_h) to minimize transmission opportunities.
- Increasing the removal or recovery rate (k) through timely isolation and effective treatment.

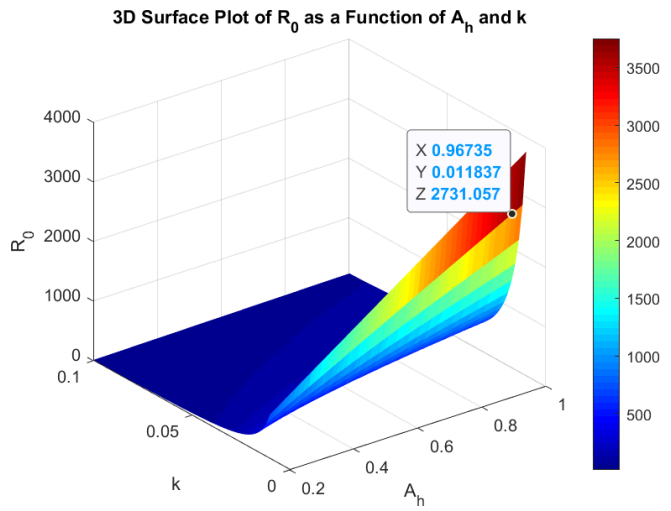

Figure 3. k, and A_h.

Low R_0 Values

Regions with low R_0 values represent environments where disease transmission is naturally limited. In these settings, the infection struggles to spread, and the disease is more likely to die out without extensive intervention.

Parameter Sensitivity

The model results indicate that the basic reproduction number (R_0) is highly sensitive to variations in the parameter k, especially at lower values. This sensitivity emphasizes the importance of:

- Enhancing removal or recovery processes to reduce the infectious period.
- Implementing effective strategies that increase k, thereby decreasing the likelihood of sustained or recurring infections.

7 Sensitivity Analysis of R_0

In this study, the sensitivity analysis of the basic reproduction number (R_0) with respect to the model parameters plays a crucial role. It allows us to identify the key factors that significantly influence the transmission and control of the disease. This section examines the sensitivity of several important parameters in the Rabies virus model, as defined in equation 1. The objective is to determine the relative importance of each parameter in relation to R_0 and to understand how changes in these parameters affect the disease dynamics. The method developed by Younas *et al.* [31] is employed to compute the sensitivity indices. The general expression for the sensitivity index of R_0 with respect to a parameter p is given by:

$$X_\theta^{R_0} = \frac{\partial R_0}{\partial \theta} \times \frac{\theta}{R_0}, \tag{10}$$

$$\theta \in \{\alpha_1, \alpha_2, \alpha_3, \beta, \delta_1, \delta_2, \delta_3, \gamma_1, \gamma_3, \kappa, \mu, A_h\} \tag{11}$$

We calculate 10 for each parameter in 11;

$$\begin{cases}
X_{A_h}^{R_0} = 1 \\
X_{\beta}^{R_0} = 1 \\
X_{\alpha_1}^{R_0} = \dfrac{\alpha_1(M_1 - \alpha_1\alpha_2)}{M_2} \\
X_{\alpha_2}^{R_0} = \dfrac{\alpha_2(M_1 - \alpha_1\alpha_2)}{M_2} \\
X_{\alpha_3}^{R_0} = \dfrac{\alpha_3(M_1 - \alpha_1\alpha_2)}{M_2} \\
X_{\delta_1}^{R_0} = \dfrac{\delta_3 C_1 - \big(C_2 M_3 - \alpha_1\alpha_2 M_4\big)}{M_5^2} \\
X_{\delta_2}^{R_0} = \dfrac{\delta_2(M_1 - \alpha_1\alpha_2)}{M_2} \\
X_{\delta_3}^{R_0} = \dfrac{\delta_3(M_1 - \alpha_1\alpha_2)}{M_2} \\
X_{\gamma_1}^{R_0} = \dfrac{\gamma_1(M_1 - \alpha_1\alpha_2)}{M_2} \\
X_{\gamma_3}^{R_0} = -\dfrac{\alpha_1\alpha_2}{M_2} \\
X_{K}^{R_0} = -\dfrac{\beta A_h M_6}{M_7 - \alpha_1\alpha_2} \\
X_{m}^{R_0} = -\dfrac{\beta A_h M_8}{M_9 - \alpha_1\alpha_2}
\end{cases} \tag{12}$$

where $M_1 = (K+m)(K+\gamma_1+\delta_1+\delta_2)(K+\gamma_3+\delta_3)(\alpha_1+K)(\alpha_2+\alpha_3+K)$,

$M_2 = \beta A_h(\alpha_2+\alpha_3+K)\big(K\delta_2+\gamma_3\delta_2+\delta_1\delta_3+\delta_2\delta_3\big)$,

$M_3 = (\alpha_1+K)^2(\alpha_2+\alpha_3+K)^2$,

$M_4 = (K+m)(K+\gamma_3+\delta_3)(\alpha_1+K)(\alpha_2+\alpha_3+K)$,

$M_5 = \beta A_h(\alpha_2+\alpha_3+K)\big(K\delta_2+\gamma_3\delta_2+\delta_1\delta_3+\delta_2\delta_3\big)$,

$M_6 = \delta_2(\alpha_2+\alpha_3+2K)+\gamma_3\delta_2+\delta_1\delta_3+\delta_2\delta_3$,

$M_7 = (K+m)(K+\gamma_1+\delta_1+\delta_2)(K+\gamma_3+\delta_3)(\alpha_1+K)(\alpha_2+\alpha_3+K)$,

$M_8 = (\alpha_2+\alpha_3+K)\big(K\delta_2+\gamma_3\delta_2+\delta_1\delta_3+\delta_2\delta_3\big)$,

$M_9 = (K+m)^2(K+\gamma_1+\delta_1+\delta_2)(K+\gamma_3+\delta_3)(\alpha_1+K)(\alpha_2+\alpha_3+K)$.

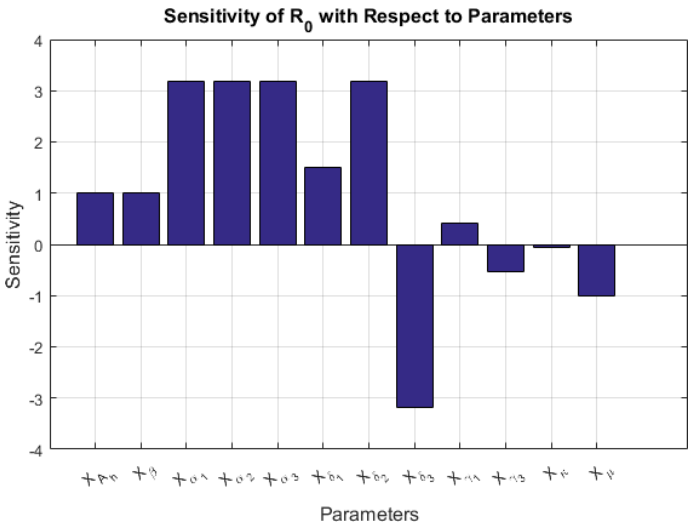

Figure 4. Bar-graph.

Discussion

As shown in Figure 4, the bar graph provides a clear and effective visualization of the sensitivity of the basic reproduction number (R_0) with respect to different model parameters such as α_1, δ_1, γ_1, and others. The analysis reveals that the height of each bar represents the degree of sensitivity of R_0 to variations in that particular parameter. Parameters associated with taller bars have a stronger influence on R_0, implying that even small changes in their values can lead to considerable variations in the reproduction number. The parameters with the greatest bar heights are identified as the most influential in determining R_0. For instance, if X_{α_1}, X_{δ_1}, and X_κ exhibit the tallest bars, they play a dominant role in shaping the transmission dynamics of the disease. On the other hand, bars extending below the zero line correspond to parameters with negative sensitivity values. This indicates that an increase in such parameters leads to a decrease in R_0, while their reduction would result in an increase in R_0. The bar graph also allows for a comparative assessment of the relative importance of the parameters. Parameters with similar sensitivity magnitudes exert comparable effects on R_0, highlighting their collective contribution to disease transmission. Understanding these relationships provides important insights into the structural behavior of the model and the mechanisms that drive infection dynamics. In conclusion, the sensitivity analysis identifies the parameters most critical in determining the basic reproduction number R_0. Recognizing these key parameters is essential for guiding public health interventions and resource allocation. For example, if κ, which may represent the transmission or contact rate, shows high sensitivity, then reducing this rate through control strategies such as vaccination, isolation, or behavioral modification becomes vital for limiting disease spread. Hence, the results of this analysis contribute to a better understanding of the model's dynamics and support the development of targeted and effective epidemic control measures.

8 Local Stability of Disease-Free Equilibrium Point

The local stability of system (1) at the disease-free equilibrium point

$$E_0 = (S^0, E^0, T^0, V^0, B^0, P^0, R^0)$$

is analyzed, where
$E_0 = \frac{(\alpha_2+\alpha_3+K)V^0}{\alpha_1}$, 0, 0, $\frac{\alpha_1 A_h}{((\alpha_1+K)(\alpha_2+\alpha_3+K)-\alpha_1\alpha_2)}$, 0, 0, 0).

The Jacobian matrix of system (1) evaluated at E_0 is given by

$$J_E = \begin{pmatrix} -A_1 & 0 & 0 & \alpha_2 & 0 & 0 & \eta \\ 0 & -A_2 & \beta S^0 & \alpha_3 & 0 & 0 & 0 \\ 0 & \delta_2 & -A_3 & 0 & 0 & \delta_3 & 0 \\ \alpha_1 & 0 & 0 & -A_4 & 0 & 0 & 0 \\ 0 & \gamma_1 & 0 & 0 & -A_5 & 0 & 0 \\ 0 & \delta_1 & 0 & 0 & 0 & -A_6 & 0 \\ 0 & 0 & 0 & 0 & \gamma_2 & \gamma_3 & -A_7 \end{pmatrix}, \tag{13}$$

where

$$A_1 = \alpha_1 + K, \quad A_2 = Z_3, \quad A_3 = K+m, \quad A_4 = Z_4,$$
$$A_5 = K+\gamma_3, \quad A_6 = Z_5, \quad A_7 = K+\eta.$$

where

$$Z_4 = \alpha_2+\alpha_3+K, \qquad Z_5 = \delta_3+\gamma_3+K.$$

The eigenvalues of J_E are

$$\lambda_1 = -(\alpha_1+K), \quad \lambda_2 = -(K+m), \quad \lambda_3 = -(K+\eta),$$
$$\lambda_4 = -(\delta_3+\gamma_3+K), \quad \lambda_5 = -(K+\gamma_3),$$

which are all negative, since the parameters are positive.

The remaining eigenvalues arise from the reduced subsystem involving the infected classes, represented by

$$J_{1E} = \begin{pmatrix} A_8 & -\alpha_3(K+m) \\ \alpha_1\eta\gamma_2\gamma_1 + (K+\gamma_3)\alpha_1\eta\gamma_1\delta_1 & -Z_6 \end{pmatrix},$$

where

$$Z_6 = (\delta_3 + \gamma_3 + K)(K + \eta)(\alpha_1\alpha_2 - (\alpha_2 + \alpha_3 + K)).$$

$$A_8 = -(\delta_2\beta S^0 + (K + m)(\delta_1 + \delta_2 + \gamma_1 + K)).$$

Theorem: 1 *The disease-free equilibrium point E_0 of system (1) is locally asymptotically stable if $R_0 < 1$ and unstable if $R_0 > 1$. [31]*

proof: To ensure local stability of the disease-free equilibrium, it is sufficient to show that the trace of J_{1E} is negative and its determinant is positive. The trace of J_{1E} is given by

$$\mathrm{Tr}(J_{1E}) = -\big[(\delta_2\beta S^0 + (K+m)(\delta_1+\delta_2+\gamma_1+K)) - Z_6\big] < 0,$$

and the determinant is $\det(J_{1E}) = \big[(\delta_2\beta S^0 + (K + m)(\delta_1 + \delta_2 + \gamma_1 + K))Z_6 - \alpha_3(K + m)(\alpha_1\eta\gamma_2\gamma_1 + (K + \gamma_3)\alpha_1\eta\gamma_1\delta_1)\big] > 0.$

If both conditions hold, all eigenvalues of J_{1E} have negative real parts. According to the Routh–Hurwitz stability criterion, these inequalities are satisfied if and only if the basic reproduction number $R_0 < 1$. Therefore, the disease-free equilibrium E_0 is locally asymptotically stable when $R_0 < 1$ and unstable when $R_0 > 1$.

8.1 Global Stability of the Disease-Free Equilibrium

The global stability of the disease-free equilibrium (DFE) is analyzed following the approach presented by H. Younas [31]. The model system (1) can be written in the general form:

$$\begin{cases} \dfrac{dD}{dt} = F(D, Q), \\ \dfrac{dQ}{dt} = G(D, Q), \qquad G(D, 0) = 0, \end{cases} \tag{14}$$

where $D \in \mathbb{R}^m$ represents the number of uninfected compartments, and $Q \in \mathbb{R}^n$ represents the number of infected compartments. The disease-free equilibrium is denoted by $E^0 = (D^0, 0)$. To guarantee the global asymptotic stability (GAS) of the DFE, the following two conditions must be satisfied:

$[(H_1)]$ For the subsystem $\dfrac{dD}{dt} = F(D, 0)$, the equilibrium point D^0 is globally asymptotically stable (GAS). $[(H_2)]$ The function $G(D, Q)$ can be expressed as

$$G(D, Q) = X_1 Q - \hat{G}(D, Q),$$

where $\hat{G}(D, Q) \geq 0$ for all $D, Q \in \Gamma$, and $X_1 = A$ is a Metzler matrix (i.e., a matrix with non-negative off-diagonal entries). Here, Γ denotes the biologically feasible

Theorem: 2 *In the event that $R < l$, the disease-free equilibrium point $E_0 = (B^0, 0)$ is globally asymptotically stable; otherwise, it is unstable [31].*

proof: The syntax for the rabies model system 18 is as follows: $D = (S, V, B, P, R), Q = (E, I)$ and $E_0 = \left(\frac{(\alpha_2+\alpha_3+K)V^0}{\alpha_1}, 0, 0, \frac{\alpha_1 A_h}{((\alpha_1+K)(\alpha_2+\alpha_3+K)-\alpha_1\alpha_2)}, 0, 0, 0\right)$ now we have

$$\frac{dD}{dt} = \begin{pmatrix} A_h + \alpha_2 V + \eta R - (\alpha_1 + K)S \\ \alpha_1 S - (\alpha_2 + \alpha_3 + K)V \\ \gamma_1 E - (\gamma_3 + K)B \\ \delta_1 E - (\delta_3 + \gamma_3 + K)P \\ \gamma_3 P + \gamma_2 B - (K + \eta)R \end{pmatrix} \tag{15}$$

At the equilibrium point of no sickness, we obtain:

$$\frac{dD}{dt} = \begin{pmatrix} A_h + \alpha_2\left(\frac{(\alpha_2+\alpha_3+K)V^0}{\alpha_1} - W_1\right) \\ (\alpha_2 + \alpha_3 + K)V^0\alpha_1 - W_2 \\ 0 \\ 0 \\ 0 \end{pmatrix} \tag{16}$$

where $W_1 = (\alpha_1 + K)\frac{\alpha_1 A_h}{(\alpha_1+K)(\alpha_2+\alpha_3+K)-\alpha_1\alpha_2}$
$W_2 = (\alpha_2 + \alpha_3 + K)\frac{\alpha_1 A_h}{(\alpha_1+K)(\alpha_2+\alpha_3+K)-\alpha_1\alpha_2}$

$F(D^0, 0)$ has a unique equilibrium point $D^0 = \left(\frac{(\alpha_2+\alpha_3+K)V^0}{\alpha_1}, \frac{\alpha_1 A_h}{((\alpha_1+K)(\alpha_2+\alpha_3+K)-\alpha_1\alpha_2)}\right)$ which is asymptotically stable globally. For this reason, (H_1) holds. Regarding condition two (H_2)

$$G(X, Q) = \begin{pmatrix} \beta SI + \alpha_3 V - (\delta_1 + \delta_2 + \gamma_1 + K)E \\ \delta_2 E + \delta_3 P - (K + m)I \end{pmatrix} \tag{17}$$

Then we get

$$X = A_1(D^0, 0) = \begin{pmatrix} -(\delta_1 + \delta_2 + \gamma_1 + K) & \beta S^0 \\ \delta_2 & -(K + m) \end{pmatrix}$$

Now, it is clear that the Matrix X is M-Matrix since its off diagonal element are non negative. Hence, $\hat{G}(D, Q) = X_1 A - G(D, Q)$ equals to

$$\hat{G}(X, Q) = \begin{pmatrix} \beta SI + \alpha_3 V - (\delta_1 + \delta_2 + \gamma_1 + K)E \\ \delta_2 E + \delta_3 P - (K + m)I \end{pmatrix} \begin{pmatrix} E \\ I \end{pmatrix}$$

$$- \begin{pmatrix} \beta SI + \alpha_3 V - (\delta_1 + \delta_2 + \gamma_1 + K)E \\ \delta_2 E + \delta_3 P - (K + m)I \end{pmatrix}$$

$$\hat{G}(X, Q) = \begin{pmatrix} \beta(S^0 - S) - (\delta_1 + \delta_2 + \gamma_1 + K) \\ 0 \end{pmatrix}.$$

Since it clear that $S^0 > S$ and it is clear that $\hat{G}(D,Q) \geq 0$, and $D^0 = \left(\frac{(\alpha_2+\alpha_3+K)V^0}{\alpha_1}, \frac{\alpha_1 A_h}{((\alpha_1+K)(\alpha_2+\alpha_3+K)-\alpha_1\alpha_2)}\right)$, is globally asymptotically stable.

9 Endemic Equilibrium Point

An *endemic equilibrium point* (*EEP*) refers to a steady-state condition in which a disease persists in the population at a constant level over time. At this equilibrium, the number of new infections is exactly balanced by the number of recoveries and disease-induced deaths, so that the total number of infected individuals remains constant. This concept plays a central role in epidemiological modeling, as it provides insight into the long-term persistence and behavior of infectious diseases within a population.

At the endemic equilibrium, all derivatives of the system vanish, i.e.,

$$\frac{dS}{dt} = \frac{dE}{dt} = \frac{dI}{dt} = \frac{dV}{dt} = \frac{dB}{dt} = \frac{dP}{dt} = \frac{dR}{dt} = 0,$$

and the corresponding equilibrium values $(S^*, E^*, I^*, V^*, B^*, P^*, R^*)$ satisfy the following system:

$$\begin{cases} S^* = \dfrac{A_h + \alpha_2 V^* + \eta R^*}{\alpha_1 + K}, \\ E^* = \dfrac{\beta S^* I^* + \alpha_3 V^*}{\delta_1 + \delta_2 + \gamma_1 + K}, \\ I^* = \dfrac{\delta_2 E^* + \delta_3 P^*}{K + m}, \\ V^* = \dfrac{\alpha_1 S^*}{\alpha_2 + \alpha_3 + K}, \\ B^* = \dfrac{\gamma_1 E^* \beta S^* I^* + \alpha_3 V^*}{(\delta_1 + \delta_2 + \gamma_1 + K)(\gamma_3 + K)}, \\ P^* = \dfrac{\delta_1 E^* \beta S^* I^* + \alpha_3 V^*}{(\delta_1 + \delta_2 + \gamma_1 + K)(\delta_3 + \gamma_3 + K)}, \\ R^* = \dfrac{\gamma_3 P^* + \gamma_2}{K + \eta} \cdot \dfrac{\gamma_1 E^* \beta S^* I^* + \alpha_3 V^*}{(\delta_1 + \delta_2 + \gamma_1 + K)(\gamma_3 + K)}. \end{cases} \quad (18)$$

9.1 Global Stability of the Endemic Equilibrium Point

To establish the global stability of the endemic equilibrium point B^0, the Lyapunov function proposed by H. Younas [31] is employed. The Lyapunov stability approach provides a rigorous mathematical tool for analyzing the asymptotic behavior of nonlinear dynamical systems. Let $V(x)$ be a continuously differentiable Lyapunov function defined in a suitable positively invariant region of the system. If the time derivative of $V(x)$ along the trajectories of the system satisfies

$$\frac{dV}{dt} < 0,$$

for all $x \neq B^0$, then $V(x)$ is said to be a Lyapunov function for the system. Consequently, the endemic equilibrium point B^0 is *globally asymptotically stable* (G.A.S.) within the biologically feasible region. In summary, the negativity of $\frac{dV}{dt}$ ensures that all trajectories of the system approach the endemic equilibrium B^0 as $t \to \infty$, confirming that the disease persists at a stable endemic level under the given conditions.

Theorem: 3 *For the Model System, the rabies epidemic has a distinct endemic equilibrium point B^*, which is globally asymptotically stable if $R_0 > 1$ and unstable otherwise.* [25]

proof:
Examining the quadratic Lyapunov function by itself

$$V(y_1, y_2, y_3, ..., y_n) = \sum_{i=1}^{n} \frac{1}{2} [y_i - y_i^*]^2,$$

where y^* is the endemic equilibrium point and y_i is the population of the ith compartment. The following is a positive definite function for the model system (1).

$$V(S,\ E,\ I,\ V,\ B,\ P,\ R) = \sum_{i=1}^{n} \frac{1}{2} [y_i - y_i^*]^2, \quad (19)$$

The rabies model system's Lyapunov function is thus expressed as follows:

$$V = \frac{1}{2}\Big[(S - S^*) + (E - E^*) + (I - I^*) + (V - V^*) + (B - B^*) + (P - P^*) + (R - R^*)\Big]^2. \quad (20)$$

It is evident that $V : R_+^7 \to R$ is a differentiable and continuous function. Next, the function $V(t)$ can be differentiated with respect to time to obtain:

$$\frac{dV}{dt} = \big[(S - S^*) + (E - E^*) + (I - I^*) + (V - V^*) + (B - B^*) + (P - P^*) + (R - R^*)\big]\frac{d}{dt}(S + E + I + V + B + P + R) \quad (21)$$

$$\frac{dV}{dt} = [(S+E+I+V+B+P+R)- (S^*+E^*+I^*+V^*+B^*+P^*+R^*)] \frac{d}{dt}(S+E+I+V+B+P+R) \quad (22)$$

But

$$\frac{dV}{dt}(S+E+I+V+B+P+R) = \Lambda_h - KN - mI \quad (23)$$

$$\Lambda_h - KN^* - mI^* = 0 \Rightarrow \Lambda_h - \mu(S^*+E^*+P^*+I^*+V^*+R^*) - mI^*$$

$$(S^*+E^*+P^*+I^*+V^*+R^*) = \frac{\Lambda_h - KI^*}{K} \quad (24)$$

Now put 23 and 24 in 22 into gives $\frac{dV}{dt}$

$$\frac{dV}{dt} = \left[N(t) - \frac{\Lambda_h - KI^*}{\mu}\right][\Lambda_h - KN - mI],$$

$$\frac{dV}{dt} = \left[N(t) - \frac{\Lambda_h - mI^*}{\mu}\right] - K\left[N(t) - \frac{\Lambda_h - mI}{\mu}\right],$$

$$\Rightarrow \frac{dV}{dt} = -K\left[N(t) - \frac{\Lambda_h - mI^*}{K}\right]\left[N(t) - \frac{\Lambda_h - mI}{\mu}\right],$$

$$\Rightarrow \frac{dV}{dt} \leq -K\left[N(t) - \frac{\Lambda_h - mI^*}{\mu}\right]\left[N(t) - \frac{\Lambda_h - mI^*}{K}\right],$$

That is

$$\frac{dV}{dt} \leq -K\left[N(t) - \frac{\Lambda_h - mI^*}{K}\right]^2, \quad (25)$$

Consequently, $\frac{dV}{dt} < 0$ is evident, indicating that B^0, the Endemic Equilibrium Point, is globally asymptotically stable.

10 Numerical Simulations

Numerical simulations were carried out using the MATLAB 2018a software with the `ODE45` solver, which employs a combination of the fourth- and fifth-order Runge–Kutta (RK5) methods. This solver has proven effective in accurately representing the dynamics of the rabies transmission model. The initial conditions used in the simulation are: $S = 500$, $V = 0$, $E = 100$, $I = 100$, and $R = 0$. These values were chosen to illustrate the dynamic behavior of the system under realistic conditions. Figure 5 illustrates the temporal evolution of the various compartments of the rabies model. The results show a rapid decline in the number of susceptible animals during the early stages of the simulation. This decline can be attributed to two main factors:

- The increase in vaccination coverage at a constant rate of 0.1, corresponding to a vaccine effectiveness of $\alpha_1 = 0.1$. Vaccination reduces the susceptibility of animals by providing immunity against rabies.
- The transmission of infection through contact with infected animals, which further decreases the susceptible population as new infections occur.

These processes, illustrated graphically, provide valuable insight into the early effects of vaccination and disease transmission dynamics within the rabies population. In accordance with the One Health framework proposed by H. Younas [31], the results highlight the crucial role of effective vaccination strategies and the importance of controlling infection spread to manage rabies effectively in animal populations.

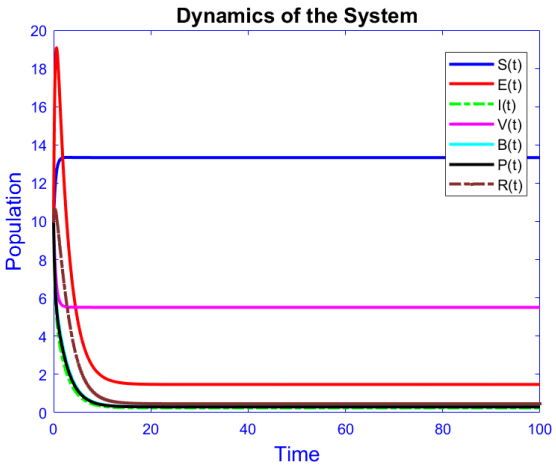

Figure 5. Animal population evolution over time.

10.1 Impact of Transition Rate (m) on Infection Dynamics

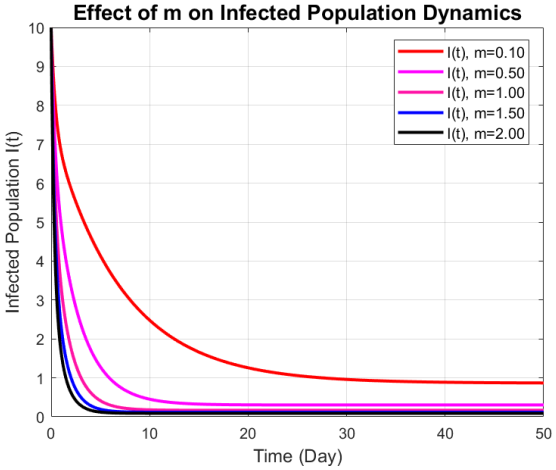

Figure 6. Effect of transition rate m on infected population $I(t)$.

This section analyzes how different values of the transition rate m affect the infection dynamics over time. The parameter m represents the rate at which infected individuals progress to more severe stages or experience disease-induced mortality. By plotting the infected population $I(t)$ for varying values of m, we examine the influence of this rate on the infection peak, duration, and overall prevalence.

As shown in Figure 6, increasing the value of m leads to a significant amplification of infection levels during the early epidemic phase. Higher values of m result in a more rapid rise in the number of infected individuals, reaching an earlier and higher peak compared to lower values. This indicates that faster disease progression accelerates the spread of infection within the population.

Conversely, lower values of m produce a slower, more prolonged infection curve with a reduced peak magnitude. The findings demonstrate that m plays a critical role in determining the temporal pattern and intensity of the epidemic.

10.2 Effect of Transmission Rate (β) on Infection Dynamics

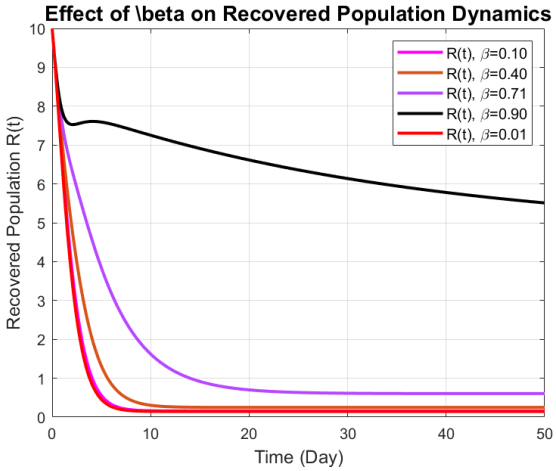

Figure 7. Effect of transmission rate β on infected population $I(t)$.

Higher values of β increase the transmission rate from susceptible (S) to exposed (E) individuals, leading to a faster rise in the number of infected individuals $I(t)$. This results in a sharper and earlier infection peak, as susceptible individuals are more rapidly exposed and infected. The analysis reveals that β strongly influences infection dynamics: higher β values produce faster and higher peaks in $I(t)$, while lower values yield a slower and more controlled infection trajectory (see Figure 7). Understanding the effect of β is essential for developing effective control measures to manage disease spread and reduce peak infection levels.

10.3 Effect of Transmission Rate β on Recovered Population $R(t)$

The transmission rate β significantly influences the dynamics of the recovered population $R(t)$, as shown in Figure 8.

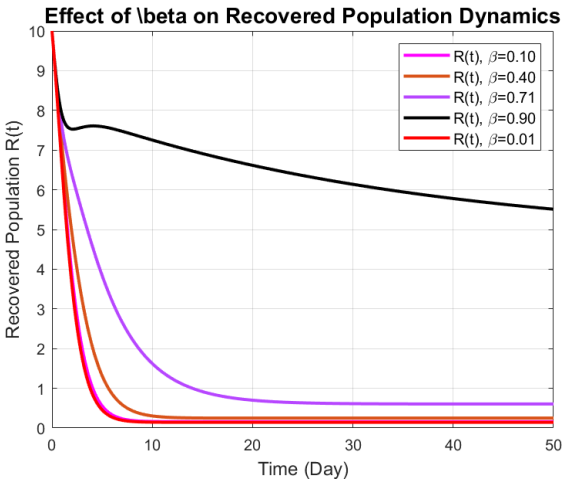

Figure 8. Effect of different β values on the recovered population $R(t)$.

High β Values ($\beta = 0.9$): A higher transmission rate accelerates infection spread, resulting in a faster accumulation of recovered individuals $R(t)$ as individuals progress through the susceptible, exposed, and infected stages. This leads to a steeper rise in the recovered population curve, with the majority of individuals reaching the recovered state earlier in the epidemic timeline.

Low β Values ($\beta = 0.009$): A lower transmission rate slows infection spread, producing a more gradual increase in the recovered population. This indicates slower disease progression, with fewer individuals reaching the recovered stage over the same time period, and a more extended recovery phase.

Overall, β has a significant effect on recovery dynamics: higher values cause faster spread and earlier recovery peaks, while lower values result in slower and more extended recovery. Controlling transmission rates through interventions such as social distancing or isolation measures is therefore crucial for managing recovery levels and reducing healthcare burden during outbreaks.

10.4 Impact of Vaccination Rates (α_1, α_2) on Disease Transmission

The parameters α_1 and α_2, representing vaccination rates, are set to 0.13 and 0.15, respectively. In the model, a portion of the susceptible population moves to the vaccinated class over time, reducing the number of individuals at risk of infection. This demonstrates how vaccination decreases disease transmission by limiting the pool of susceptible individuals (as shown in Figures 9, 10 and 11) For comparison, a simulation without vaccination is also considered, where $\alpha_1 = \alpha_2 = 0$. In this case, no immunization occurs, and the disease spreads freely in the population, leading to an increase in both exposed and infected individuals. Dashed lines in the corresponding figure represent the "no vaccination" scenario. Comparing these results highlights the effectiveness of vaccination in lowering infection peaks and controlling disease spread within the community. The dramatic reduction in infected individuals observed when vaccination and booster doses are implemented aligns with large-scale field evidence from national dog vaccination programs [24, 26]. In Mexico, sustained annual vaccination coverage above 70% led to near-elimination of canine-mediated human rabies deaths over two decades [24], while in south-east Tanzania, high vaccination coverage in domestic dogs was shown to disrupt transmission even in areas with wildlife reservoirs [26]. These real-world outcomes strongly support our model's prediction that combining primary and booster vaccination represents one of the most cost-effective and feasible strategies for achieving the WHO 2030 zero-dog-mediated-human-rabies target.

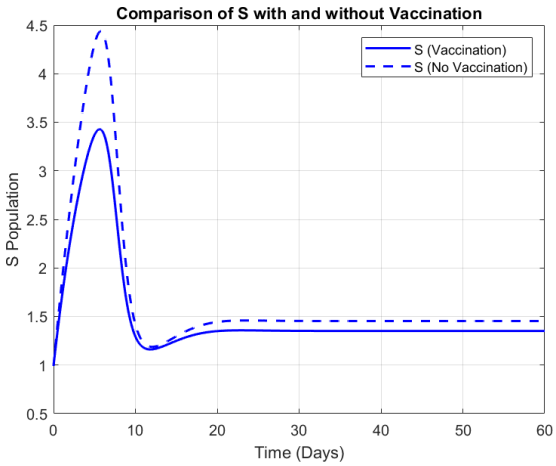

Figure 9. With vaccine and with out vaccine.

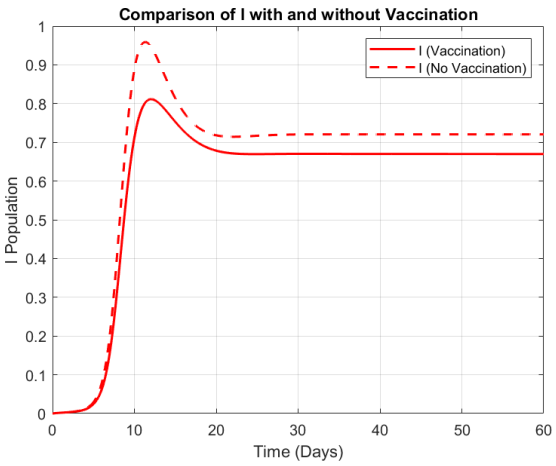

Figure 10. With vaccine and with out vaccine.

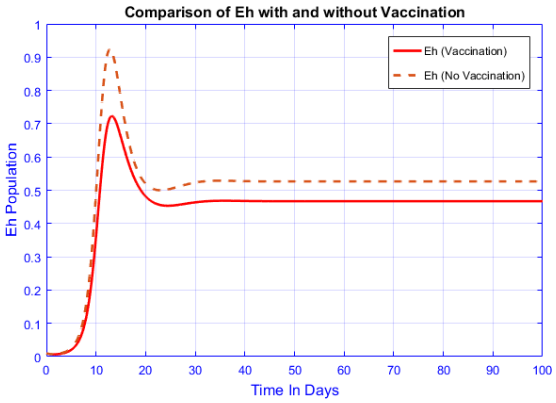

Figure 11. With vaccine and with out vaccine.

11 Conclusion

In this study, a mathematical model for the dynamics of rabies transmission was developed and analyzed by incorporating two important intervention strategies: the booster vaccination class (B) and the asymptomatic class (P). The model, formulated through a system of nonlinear differential equations, was used to derive the basic reproduction number R_0, which serves as a threshold parameter determining whether the disease persists or dies out. A sensitivity analysis of R_0 identified the key parameters that most strongly influence disease transmission. The transmission rate (β) was found to have the greatest impact, emphasizing the importance of reducing contact between susceptible and infected individuals. The stability analysis of both the disease-free and endemic equilibria showed that the disease can be eradicated when $R_0 < 1$, while it persists when $R_0 > 1$ under biologically feasible conditions. To complement the analytical results, numerical simulations were carried out using the classical Runge–Kutta method. These simulations illustrated the comparative effects of vaccination and treatment interventions. The results

clearly demonstrate that the inclusion of the booster vaccination class (B) significantly reduces the number of infected individuals compared to the scenario without vaccination. Moreover, the treatment class (P) further decreases disease burden and accelerates recovery. The analysis of varying transmission rates (β) revealed that higher values of β lead to faster and higher infection peaks, highlighting the importance of strong control measures in high-contact environments. Overall, the model demonstrates that the incorporation of booster vaccination and treatment strategies can substantially reduce the incidence of rabies. The findings provide valuable insights that can support public health programs aimed at controlling and ultimately eliminating rabies. It is worth noting that parameter uncertainty, as explored in fuzzy and crisp modeling frameworks [29], can further influence threshold conditions and control efficacy, suggesting that robust control strategies should remain effective across plausible parameter ranges.

Data Availability Statement

Data will be made available on request.

Funding

This work was supported without any funding.

Conflicts of Interest

The authors declare no conflicts of interest.

Ethical Approval and Consent to Participate

Not applicable.

References

[1] Panjeti, V. G., & Real, L. A. (2011). Mathematical models for rabies. *Advances in Virus Research, 79*, 377–395. [CrossRef]

[2] Layan, M., Dellicour, S., Baele, G., Cauchemez, S., & Bourhy, H. (2021). Mathematical modelling and phylodynamics for the study of dog rabies dynamics and control: A scoping review. *PLOS Neglected Tropical Diseases, 15*(5), e0009449. [CrossRef]

[3] Hankins, D. G., & Rosekrans, J. A. (2004). Overview, prevention, and treatment of rabies. *Mayo Clinic Proceedings, 79*(5), 671–676. [CrossRef]

[4] Demirci, E. (2014). A new mathematical approach for rabies endemy. *Applied Mathematical Sciences, 8*(2), 59–67. [CrossRef]

[5] Tulu, A. M. (2017). *Mathematical Modeling on the Impact of Infective Immigrants on the Spread of Dog Rabies* (Doctoral dissertation).

[6] Barecha, C. B., Girzaw, F., Kandi, R. V., & Pal, M. (2017). Epidemiology and public health significance of rabies. *Perspectives in Clinical Research, 5*(1), 55–67.

[7] Mumbu, A. J. (2022). *Modelling dynamics of dog rabies disease with vaccination and treatment in dog population* [Doctoral dissertation, University of Dodoma].

[8] Hampson, K., Coudeville, L., Lembo, T., Sambo, M., Kieffer, A., Attlan, M., … (2015). Estimating the global burden of endemic canine rabies. *PLOS Neglected Tropical Diseases, 9*(4), e0003709. [CrossRef]

[9] Changalucha, J., Steenson, R., Grieve, E., Cleaveland, S., Lembo, T., Lushasi, K., Mchau, G., Mtema, Z., Sambo, M., Nanai, A., … (2019). The need to improve access to rabies post-exposure vaccines: Lessons from Tanzania. *Vaccine, 37*(Suppl. 1), A45–A53. [CrossRef]

[10] Warrell, D. A. (2007). *Rabies and envenomings: a neglected public health issue: report of a consultative meeting, World Health Organization, Geneva, 10 January 2007*. World Health Organization.

[11] WHO Rabies Modelling Consortium. (2020). Zero human deaths from dog-mediated rabies by 2030: perspectives from quantitative and mathematical modelling. *Gates Open Research, 3*, 1564. [CrossRef]

[12] Fagbo, S., & Asiri, A. (2022). Sand cat rabies in Saudi Arabia: Leveraging to improve spillover surveillance and one health impact. *International Journal of Infectious Diseases, 116*, S106-S107. [CrossRef]

[13] Ruan, S. (2017). Spatiotemporal epidemic models for rabies among animals. *Infectious Disease Modelling, 2*(3), 277–287. [CrossRef]

[14] Kanankege, K. S., Errecaborde, K. M., Wiratsudakul, A., Wongnak, P., Yoopatthanawong, C., Thanapongtharm, W., ... & Perez, A. (2022). Identifying high-risk areas for dog-mediated rabies using Bayesian spatial regression. *One Health, 15*, 100411. [CrossRef]

[15] Huang, Y., & Li, M. (2020). Application of a mathematical model in determining the spread of the rabies virus: Simulation study. *JMIR Medical Informatics, 8*(5), e18627. [CrossRef]

[16] Coyne, M. J., Smith, G., & McAllister, F. E. (1989). Mathematic model for the population biology of rabies in raccoons in the mid-Atlantic states. *American Journal of Veterinary Research, 50*(12), 2148–2154.

[17] Eze, O. C., Mbah, G. E., Nnaji, D. U., & Onyiaji, N. E. (2020). Mathematical modelling of transmission dynamics of rabies virus. *International Journal of Mathematics Trends and Technology, 66*(6), 126–134. [CrossRef]

[18] Agaba, G. O. (2014). Modelling of the spread of rabies with pre-exposure vaccination of humans. *Mathematical Theory and Modeling, 4*(8), 57–63.

[19] Ruan, S. (2017). Modeling the transmission dynamics and control of rabies in China. *Mathematical Biosciences, 286*, 65–93. [CrossRef]

[20] Ndendya, J. Z., Leandry, L., & Kipingu, A. M. (2023). A next-generation matrix approach using Routh–Hurwitz criterion and quadratic Lyapunov function for modeling animal rabies with infective immigrants. *Healthcare Analytics, 4*, 100260. [CrossRef]

[21] Omame, A., Isah, M. E., & Abbas, M. (2023). An optimal control model for COVID-19, zika, dengue, and chikungunya co-dynamics with reinfection. *Optimal Control Applications and Methods, 44*(1), 170–204. [CrossRef]

[22] Agbata, C. (2025). A Mathematical Model for the Control of Ebola Virus Disease with Vaccination Effect. *Journal of Mathematical Epidemiology, 1*(1), 26-48. [CrossRef]

[23] Liu, J., Jia, Y., & Zhang, T. (2017). Analysis of a rabies transmission model with population dispersal. *Nonlinear Analysis: Real World Applications, 35*, 229–249. [CrossRef]

[24] Gonzalez-Roldán, J. F., Undurraga, E. A., Meltzer, M. I., Atkins, C., Vargas-Pino, F., Gutiérrez-Cedillo, V., & Hernández-Pérez, J. R. (2021). Cost-effectiveness of the national dog rabies prevention and control program in Mexico, 1990–2015. *PLOS Neglected Tropical Diseases, 15*(3), e0009130. [CrossRef]

[25] Kanda, K., Jayasinghe, A., Jayasinghe, C., & Yoshida, T. (2022). A regional analysis of the progress of current dog-mediated rabies control and prevention. *Pathogens, 11*(10), 1130. [CrossRef]

[26] Lushasi, K., Hayes, S., Ferguson, E. A., Changalucha, J., Cleaveland, S., Govella, N. J., & Hampson, K. (2021). Reservoir dynamics of rabies in south-east Tanzania and the roles of cross-species transmission and domestic dog vaccination. *Journal of Applied Ecology, 58*(11), 2673–2685. [CrossRef]

[27] Bornaa, C. S., Seidu, B., & Daabo, M. I. (2020). Mathematical analysis of rabies infection. *Journal of Applied Mathematics, 2020*(1), 1804270. [CrossRef]

[28] Ega, T. T., Luboobi, L. S., & Kuznetsov, D. (2015). Modeling the dynamics of rabies transmission with vaccination and stability analysis. *Journal of Applied Mathematics, 2015*, 1–12.

[29] Ndii, M. Z., Amarti, Z., Wiraningsih, E. D., & Supriatna, A. K. (2018). Rabies epidemic model with uncertainty in parameters: Crisp and fuzzy approaches. *IOP Conference Series: Materials Science and Engineering, 332*(1), 012031. [CrossRef]

[30] Jehangir, H., Ali, N., Ahmad, I., Younas, H., Ahmad, Z., & El-Agamy, R. F. (2024). Global Dynamics and Numerical Simulation of a Vaccinated Mathematical Model for Rabies Disease. *Global Journal of Sciences, 1*(1), 14-27. [CrossRef]

[31] Younas, H., Ahmad, I., Ali, N., Haq, I. U., Albalwi, M. D., Muhammad, S., & Shuaib, M. (2024). Modeling rabies dynamics: the impact of vaccination and infectious immigrants on public health. *Contemp. Math, 5*(3), 3255. [CrossRef]

Hanif Ullah received his M.Sc. degree in Mathematics from the University of Malakand and his M.Phil. degree in Mathematics from the University of Engineering and Technology (UET), Peshawar, Pakistan. His research interests lie in mathematical modeling, numerical analysis, and infectious disease dynamics. His recent work focuses on the development and stability analysis of epidemiological models incorporating vaccination and booster vaccination strategies, with numerical simulations performed using advanced computational methods. (Email: hanifullahbjr23@gmail.com)

Prof. Dr. Amjad Ali is a Professor of Mathematics in the Department of Basic Sciences and Islamiat at the University of Engineering and Technology (UET), Peshawar, Pakistan, where he currently serves as Dean of the Faculty of Architecture, Allied Sciences & Humanities. With over 27 years of academic experience, he has held various leadership roles at UET, including Head of Department and Provost of University Hostels. Dr. Ali obtained his Ph.D. and M.S. in Applied Mathematics from Ghulam Ishaq Khan Institute of Engineering Sciences and Technology, and his M.Sc. in Mathematics from the University of Peshawar, where he graduated with a gold medal. His research focuses on symmetries in general relativity, teleparallel gravity, and related areas of applied mathematics, and he has authored numerous articles in esteemed journals in these fields. (Email: ali@uetpeshawar.edu.pk)

Hazrat Younas received his B.S. in Mathematics from Abdul Wali Khan University Mardan and his M.Phil. in Mathematics from the University of Malakand, Pakistan. His research interests include mathematical modeling, numerical analysis, and infectious disease dynamics. (Email: mathsk45@gmail.com)